Materials Today Communications 27 (2021) 102244

Contents lists available at ScienceDirect

Materials Today Communications

journal homepage: www.elsevier.com/locate/mtcomm

Design of a Mg-7Li-2.6Al-0.4Si alloy with simultaneously improved strength and ductility

Zilong Zhao [a,b], Junxian Chen [a], Xin Wu [a,*], Faqian Liu [a,*]

[a] School of Chemical Engineering and Technology, Sun Yat-sen University, Zhuhai 519082, China
[b] School of Mechanical Engineering and Automation, Fuzhou University, Fuzhou 350116, China

ARTICLE INFO

Keywords:
Mg-7Li-2.6Al-0.4Si alloy
Mechanical properties
Precipitate
Grain refinement

ABSTRACT

Mg-Li alloys have been widely applied in various engineering scenarios due to the ultralight feature. One of the key factors determining the applications of Mg-Li alloys is the strengthening methods, which have received much attention. In this paper, a new Mg-7Li-2.6Al-0.4Si (all in wt.%) alloy was designed and produced to improve the mechanical performance. The simultaneously outstanding mechanical strength and ductility have been demonstrated by nano indentation and tensile test, including a yield strength of 192 MPa, tensile strength of 250 MPa and elongation of 22 %. Based on the microstructural features characterized by optical microscopy, scanning electron microscopy and transmission electron microscopy, the excellent mechanical properties were attributed to the precipitates and refined grain size. The fracture morphology was also uncovered to further explain the good mechanical performance. Overall, this work yields a new Mg-7Li-2.6Al-0.4Si alloy with excellent properties, which suggest its great potential for various applications.

1. Introduction

Magnesium (Mg) alloys, as the lightest metallic materials for structural applications, have attracted numerous interests in applications involving automotive, aerospace, 3D products, etc., due to their benefits of low density, high specific strength, large damping capacity, high specific stiffness and good castability [1]. The majority of magnesium alloy products are produced by casting processing, which usually results in pieces with poor ductility and insufficient strength, inferior formability, largely restricting the further expansion of the applications for Mg alloys. To resolve these issues, one way is to adopt the deformation techniques such as extrusion or rolling for alloy processing, which could significantly improve the strength, ductility and toughness of the alloys through grain/subgrain strengthening and dislocation density strengthening [2–6]. Meanwhile, alloying with other elements has also been an attractive way to improve the overall performance of Mg alloys.

Magnesium-Lithium (Mg-Li) alloys emerge as a more promising material system among Mg alloys due to the super lightweight, relatively high strength and good formability, which could overcome some of the drawbacks for Mg alloys, while further reduce the density [7–12]. The performance of Mg-Li alloys highly depends on the amount of Li being added. Based on the Mg-Li phase diagram, Li solid solution of BCC β-phase coexists with Mg solid solution of HCP α-phase at room temperature when the Li concentrations are in the range of 5−11 wt.% [13, 14], which could usually generate alloys with moderate strength and good ductility. However, the formation of β-phase would scarify the mechanical strength, which results in insufficient strength for some application scenarios. Therefore, substantial research effort has been made to strengthen Mg-Li alloys. Among various approaches, alloying design and deformation processing have been recognized as effective methods, and considerable research interest has been intrigued [15]. For example, Xu et al. [16] designed a lithium-rich ultra-low density (1.4 g. cm^{-3}) Mg-Li based alloy. Through a series of extrusion, heat treatment and rolling processes, a solute nanostructure in the body-centered cubic matrix was achieved, which results in the Mg-Li alloy with excellent toughness and corrosion resistance. Han et al. [17] prepared ultra-fine grained Al-Mg-Si alloys with different Mg/Si ratios by using extrusion and cold drawing. It was found that the Mg/Si ratio could determine the precipitate density as well as the inter-precipitate spacing, which further affected the strength and electrical conductivity of the alloys. Gong [18] studied the influence of extrusion pass on the microstructure and mechanical properties of Mg-12Al-0.7Si alloy through an equal channel angular extrusion (ECAP) experiment. The size of the Mg_2Si phase was discovered to be around 2∼3 μm after 8 times of ECAP processing. The

* Corresponding authors.
E-mail addresses: wuxin28@mail.sysu.edu.cn (X. Wu), liufq7@mail.sysu.edu.cn (F. Liu).

https://doi.org/10.1016/j.mtcomm.2021.102244
Received 25 October 2020; Received in revised form 1 March 2021; Accepted 8 March 2021
Available online 10 March 2021

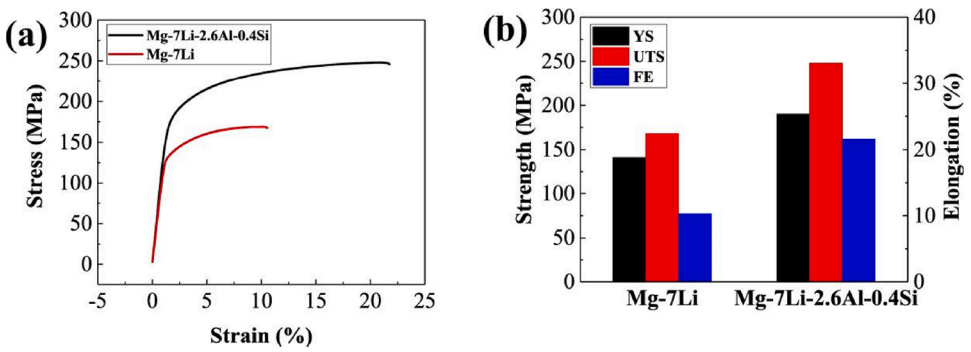

Fig. 1. Mechanical tensile properties of annealed Mg-7Li and Mg-7Li-2.6Al-0.4Si alloys. (a) Engineering stress-strain curves of annealed Mg-7Li and Mg-7Li-2.6Al-0.4Si alloys. (b) Tensile strengths and elongations of Mg-7Li and Mg-7Li-2.6Al-0.4Si alloys.

morphology was changed from the initial Chinese script shape to fine granule polygonal shape, which tended to increase the strength and elongation of the dispersed alloy. Alloying Al in Mg-Li based alloys could lead to an enhanced mechanical strength through the precipitation and solid solution strengthening [19], and alloying Si in Mg-Li alloys could further improve the tensile strength [20]. However, these methods still have some limitations, e.g., the deformation processing is usually constituted by complex procedures, and the addition of Al could only generate alloys with limited strength, and Si would bring in brittle Mg_2Si phase. Moreover, in most cases, we would like to obtain Mg-Li based alloys with simultaneously good strength and ductility, while it is hard to achieve this goal based on the current methodology.

The addition of Al-Si eutectic alloys has been demonstrated to be able to dramatically improve the tensile strength of the dual Mg-Li based alloys with a slightly reduced elongation [21]. Meanwhile, the burning loss rate could also be largely reduced [22]. The purpose of this work is to combine the deformation processing (casting + extrusion) with alloying design to achieve a Mg-Li based alloy with improved strength and ductility. A new Mg-Li based alloy, namely, Mg-7Li-2.6Al-0.4Si was designed by adding Al-Si eutectic alloy into Mg-7Li. Through optical microscopy (OM), scanning electron microscopy (SEM), electron back scattered diffraction (EBSD) analyses, energy-dispersive X-ray spectroscopy (EDS), X-ray diffraction (XRD), transmission electron microscopy (TEM), nano indentation and mechanical tensile test, the effect of addition of Al-Si eutectic alloy and extrusion on the microstructure and mechanical behavior of the newly developed alloy were investigated. The underlying strengthening and toughing mechanism have also been revealed.

2. Experimental methods

2.1. Sample preparation

The Mg-7Li and Mg-7Li-2.6Al-0.4Si alloys (all in wt.%, unless otherwise stated) were prepared by magnetic-levitation, vacuum, and high-frequency induction melting technique. Pure magnesium (≥99.95 wt%), pure lithium (≥99.95 wt%) and/or aluminum-silicon eutectic were melted under an argon atmosphere initially, and then the melt was rapidly casted into a water-cooled copper mold to form a cast rod with a dimension of Φ30 mm*60 mm. The ingot was then extruded once to form a 6 mm*12 mm plate (extruded alloys). Subsequently, all the specimens were annealed at 200 °C for 60 min (annealed alloys).

2.2. Mechanical testing

Tensile tests were conducted to evaluate the mechanical properties of the materials. For tensile tests, the specimens having a gauge length of 25 mm, width of 5.7 mm and thickness of 1.5 mm were machined from the annealed plates. The tensile test was performed on an electronic universal testing machine (CMT5205, MTS Systems Corporation, US) according to ASTM E8/E8M-2011 standard. The displacement rate was set at 0.5 mm/min. In total, five tensile tests were repeated for each sample condition to obtain good statistics of the results. The nano-indenter NanoTest Vantage with a wide accessible loading range from 10 μN up to 30 N was adopted for the micro contact mechanics testing.

2.3. Microstructural characterization

The microstructures were examined by using an optical microscope (DM-2700 P, LECIA, Germany), a scanning electron microscope (SEM, JSM-7800 F, JEOL, Japan) equipped with an Oxford electron back-scattered diffraction (EBSD) system and energy dispersive spectroscopy (EDS), and a transmission electron microscope (TEM, JEOL-2100 F, JEOL, Japan). The texture of the grains was characterized using EBSD measurement with a step size of 3 μm. The specimens for microstructure characterization were mechanically ground using silicon paper from 400# to 2000#, and etching with a reagent of 2.5 g picric +3 mL acetic acid +21 mL ethanol was adopted to reveal the microstructure. For preparation of the TEM samples, focused ion beam (FIB) polishing in a TESCAN GAIA3 FIB-SEM was applied.

3. Results and discussions

3.1. Mechanical properties of the as-processed alloys

The mechanical properties of annealed Mg-7Li and Mg-7Li-2.6Al-0.4Si alloys were depicted in Fig. 1. It is seen from Fig. 1(a) that Mg-7Li-2.6Al-0.4Si alloy presents a simultaneously much larger tensile strength and fracture strain. By further analyzing the data, the values of ultimate tensile strength (UTS), yield strength (YS) and fracture elongation (FE) were given in Fig. 1(b), which demonstrates that the addition of Al and Si leads to the increase in UTS, YS and elongation, from 168 MPa, 148 MPa and 11%–250 MPa, 192 MPa, and 22 %, respectively. It is well known that the addition of Li could improve the ductility of Mg alloys, while generate low-temperature instability and inferior strength as well due to the formation of tender and ductile β-Li phase [23]. Although Al addition could improve the strength of Mg-Li alloys, the strength of Mg-Li-Al alloys is still inferior to the conventional Mg alloys such as the AZ series [24]. Our study demonstrated that the Al-Si eutectic addition together with the deformation processing could simultaneously largely improve the mechanical strength and ductility. In previous study, Zhang et al. [25] fabricated a Mg-4Li-3(Al-Si) alloy with a UTS of 249 MPa, while the elongation reaches 6.3 %, and they also fabricated a Mg-12Li-3(Al-Si) alloy with an elongation of 26 %, while the UTS reaches 173 MPa. Thus, it is difficult to obtain a Mg-Li alloy with simultaneously good mechanical strength and ductility. The results in this work are significant in many engineering applications.

Nanoindentation test has been adopted to characterize the

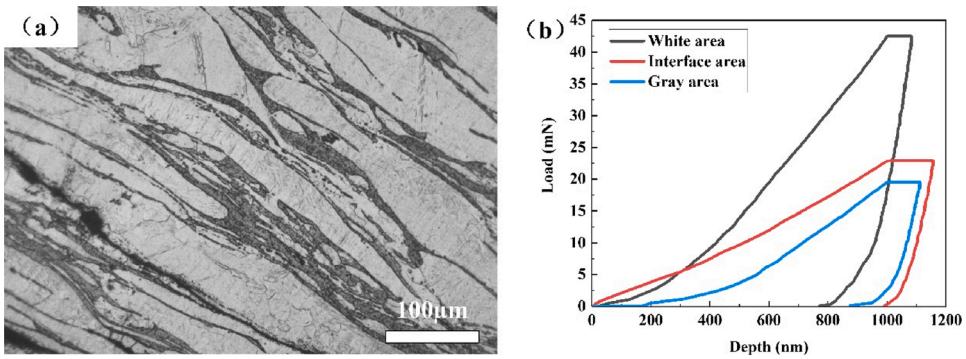

Fig. 2. OM image and nanoindentation test results of the annealed Mg-7Li-2.6Al-0.4Si alloy.

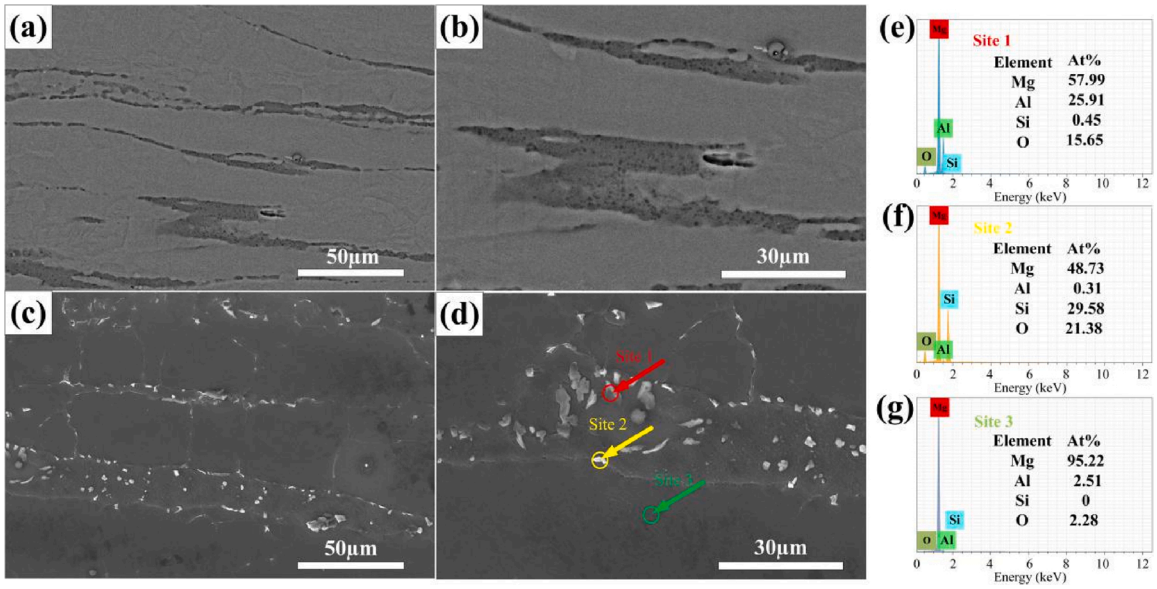

Fig. 3. Backscattered electron images and energy-dispersive X-ray spectroscopy results of annealed Mg-7Li and Mg-7Li-2.6Al-0.4Si alloys. (a-b) Backscattered electron image of Mg-7Li alloy with different magnifications. (c-d) Backscattered electron image of Mg-7Li-2.6Al-0.4Si alloy with different magnifications. (e-g) EDS results collected from the area marked by three dashed rectangles shown in (d).

mechanical behavior of the annealed Mg-7Li-2.6Al-0.4Si alloy at a micro-level. As shown in Fig. 2, the alloys are constituted by two main phases, the bright α-phase presents a higher strength and a larger Young's modulus, while the dark β-phase has a better plasticity, which is consistent with other studies [13–15]. Based on the common sense, the interface of α-phase and β-phase should exhibit mechanical properties under the combination of these two phases, i.e., enhanced ductility and reduced strength when compared to α-phase, and enhanced strength and reduced ductility when compared to β-phase. However, the plot in Fig. 2 (b) reveals that the microstructure at the interface has simultaneously enhanced strength and ductility when compared to β-phase, which maybe correlated to the abnormal mechanical properties shown in Fig. 1, and further analysis are needed to uncover the underlying mechanism of this phenomenon.

3.2. Precipitation and grain refinement

In order to explain the outstanding mechanical properties of the designed and as-processed Mg-7Li-2.6Al-0.4Si alloy, different techniques such as SEM, EDS, XRD and EBSD are adopted to characterize the microstructural features.

Fig. 3 shows backscattered electron image and energy-dispersive X-ray spectroscopy results of the annealed Mg-7Li and Mg-7Li-2.6Al-0.4Si alloys. The pale grey areas were HCP-structured α-Mg phase while the dark grey areas were BCC-structured β-Li phase. The precipitates with white contrast were observed for Mg-7Li-2.6Al-0.4Si alloy (Fig. 3(c) and Fig. 3(d)) while no precipitates were observed for Mg-7Li (Fig. 3(a) and Fig. 3(b)). Thus, the precipitates were generated due to the addition of Al and Si. These precipitates lie around the grain boundary of the alloy, and the typical size of precipitates is about 1 μm. To reveal the detailed information of these precipitates, EDS spot analysis were conducted on three sampling areas, including the dark precipitated phase (site 1), the bright precipitated phase (site 2), and the matrix (site 3). The Al content in the dark precipitated phase was 25.91 % (Fig. 3(e)), indicating that the precipitated phase was an aluminum-rich phase. The O content of 15.65 % demonstrates that the aluminum-rich phase was oxidized and appeared to be dark black, as reported in Ref. [26]. For the white bright precipitates shown in Fig. 3(f), the Al content was 0.31 % and the Si content was 29.58 %, which means that the precipitated phase is a Si-rich phase. It has been reported that the addition of Si in Mg alloys could result in the formation of white bright Mg_2Si precipitate phase with fish-bone-shaped or Chinese-character-shaped [27], which is similar as the information in this study. The bright Mg_2Si phase was also demonstrated as the only Si-rich phase in Mg-xLi-3(Al-Si) alloys [25], further proving that Si-rich phase in this study should be Mg_2Si. These micro-sized fine Al-based and Si-based precipitates were mainly dispersed around the grain boundary to reduce the grain size of the alloys, which could generate significant strengthening effect on the alloys

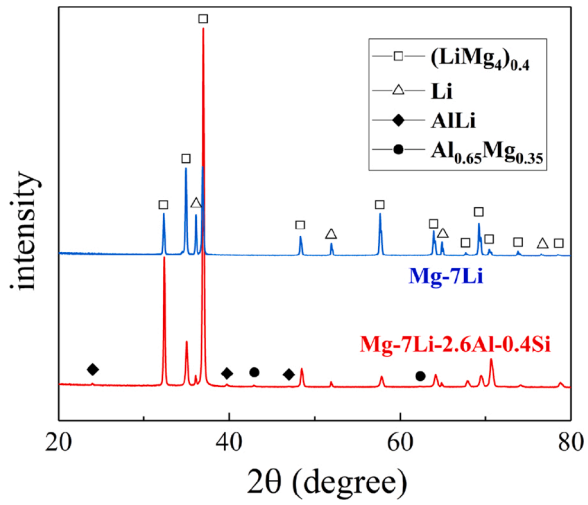

Fig. 4. XRD patterns of annealed Mg-7Li and Mg-7Li-2.6Al-0.4Si alloys.

[25]. For the matrix shown in Fig. 3(g), there are no precipitates formed. The matrix has an Al content of 2.51 %, which could generate the effect of solid solution strengthening in Mg matrix, as indicated in Ref. [28].

Fig. 4 shows the XRD patterns of as-annealed Mg-7Li and Mg-7Li-2.6Al-0.4Si alloys. The diffraction results showed that for both alloys, α-phase ($LiMg_4$) and β-Li phase were present, which is consistent with the features of Mg-Li alloys that the lattice changed from HCP to BCC when the Li content exceeds 5.5 %. The missing of Li-phase in EDS is because Li has the very low energy of characteristic radiation, not easy to detect. Meanwhile, two other phases, namely AlLi and $Al_{0.65}Mg_{0.35}$ phases, were also observed in the designed Mg-7Li-2.6Al-0.4Si alloy, which reveals the existence of AlLi phase and $Al_{0.65}Mg_{0.35}$ phase in the dark precipitates as shown in Fig. 3(e). It was also reported in other papers that the addition of Al could lead to remarkable age hardening of Mg-Li alloys due to the formation of Al-Li and Mg-Al precipitates, for which the visible precipitates are mainly dispersed at grain boundaries [29]. Zhang et al. demonstrated that alloying with Al-Si eutectic caused the formation of Mg_2Si and Mg-Al phase for Mg-4Li alloy [30], and alloying with Al-Si eutectic cause the formation of different types of Al-Li precipitates (Al_3Li, AlLi and Li_3Al_2) and Mg_2Si phase for Mg-xLi alloys (x = 4, 8 and 12 wt.%) [25]. The diffraction peak of Mg_2Si phase was not observed due to the low Si content (0.4 %). As a result of the low Si content, the coarse fish-bone-shaped or Chinese-character-shaped Mg_2Si phase was not formed, which ensures the improvement of the strength and plasticity of the alloy. It has been reported previously that the plasticity of the Mg alloys would be significantly reduced if the Si content exceeds 0.6 % [31]. Thus, the amount of Si should be controlled to be below 0.6 %. Our results demonstrated that within this Si amount, fine Mg_2Si、AlLi、$Al_{0.65}Mg_{0.35}$ precipitates could be generated, resulting in much improved strength and ductility.

The EBSD grain orientation images and the grain size analysis for Mg-7Li-2.6Al-0.4Si alloy are depicted in Fig. 5, in which the recrystallized fractions are extracted from EBSD data based on the concept proposed by Tarasiuk [32]. Fig. 5(a) shows that most of the grains were close to the red color, which indicated a strong basal texture ((0001) orientation). There are fine grains with size less than 10 μm and large grains with size of 20−30 μm existing in the microstructure of Mg-7Li-2.6Al-0.4Si alloy. Actually, the majority of grains have a grain size of 2−3 μm, as shown in Fig. 5(b). The formation of fine grains in Mg-7Li-2.6Al-0.4Si alloy is induced by the addition of Al and Si

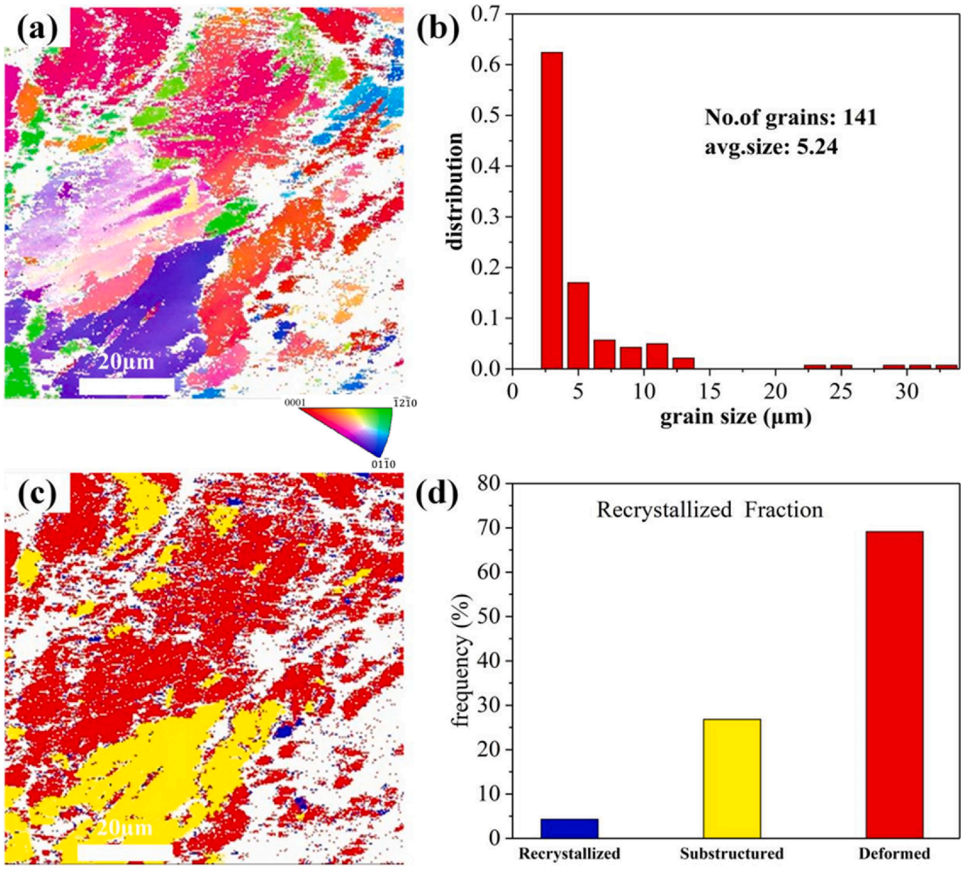

Fig. 5. EBSD testing results of annealed Mg-7Li-2.6Al-0.4Si alloy. (a) Grain orientation image. (b) Grain size distribution. (c) Dynamic recrystallization distribution. (d) Fraction of recrystallized grains.

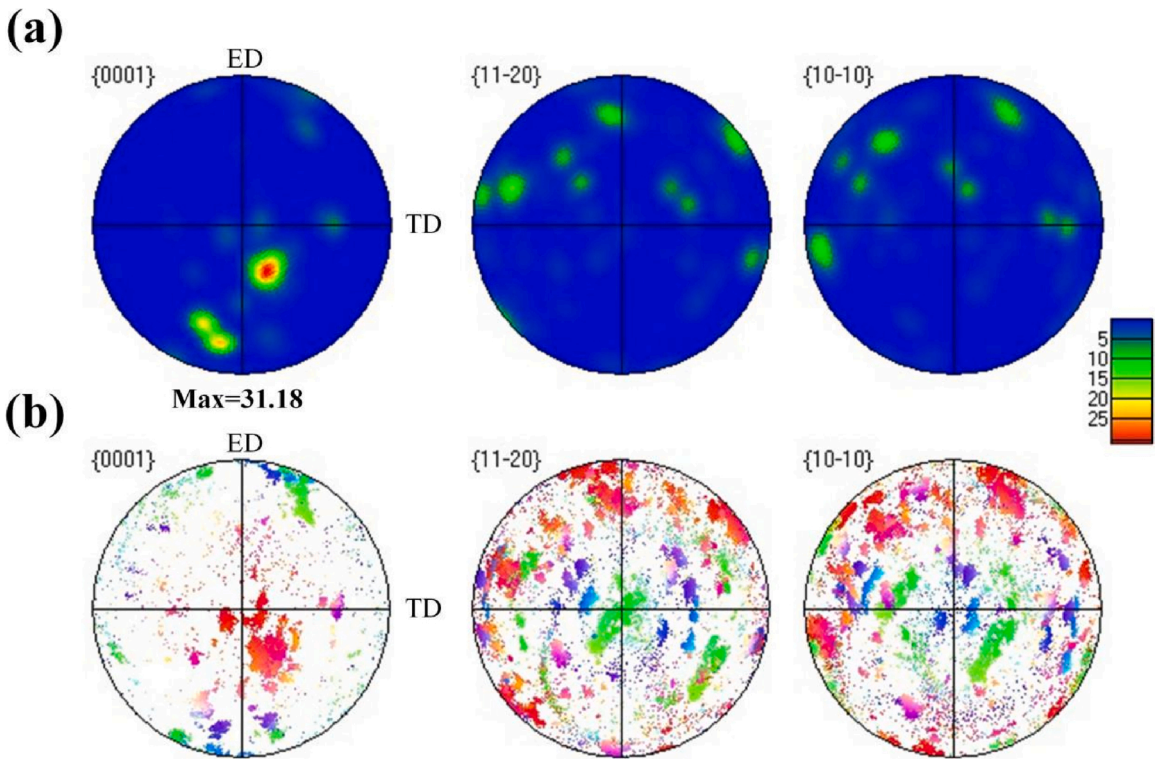

Fig. 6. (0001) Pole figures of as-annealed Mg-7Li-2.6Al-0.4Si alloy. (a) Pole figures. (b) Inverse pole figures.

elements. It is said the Al-Si eutectic alloy could promote the nucleation of new grains, and the precipitated particles could hinder the growth of grains as well [33]. From Fig. 5(b), it is also obvious that there are grains at different size levels in Mg-7Li-2.6Al-0.4Si alloy, which contributes to an average grain size of 5.24 μm. This fine grain-dominated mixed crystal structure allows Mg-7Li-2.6Al-0.4Si alloy to maintain high mechanical strength while still having good elongation, and the addition of Li makes the alloy lighter and denser. Fig. 5(c) shows the grain orientation regarding to the dynamic recrystallization, where the red areas represent deformed grains, the yellow areas represent substructure grains, and the blue areas represent dynamic recrystallized grains. It is seen that the deformed grains dominate in the as-processed Mg-7Li-2.6Al-0.4Si alloy, while there are only a few recrystallized grains appeared at the junctions of tiny grains. The frequency of each type of grains as shown in Fig. 5(d) also indicates a small recrystallized fraction. During the deformation and annealing process, the fine

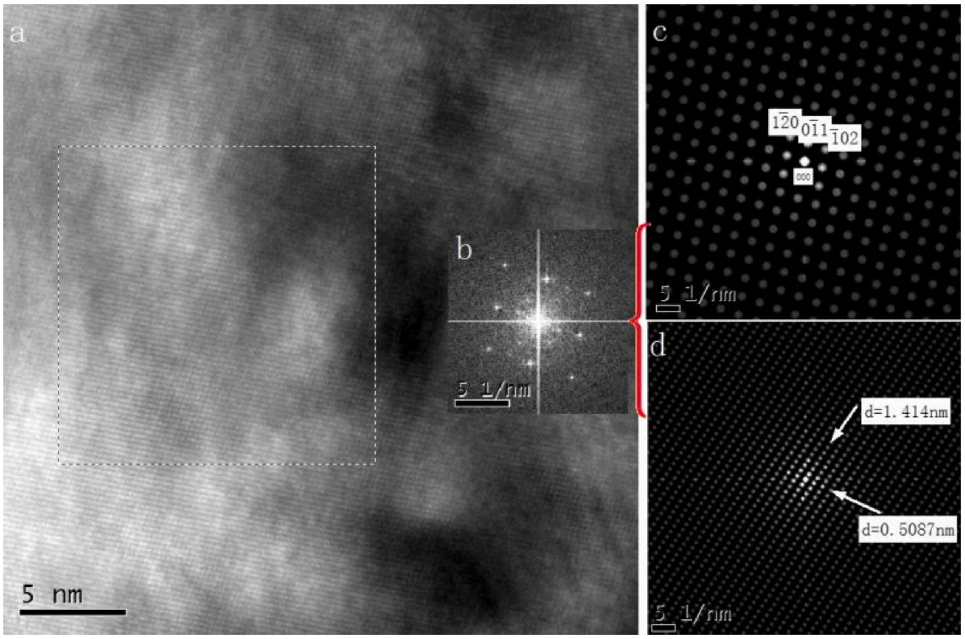

Fig. 7. HRTEM images of a spherical precipitate in the as-annealed Mg-7Li-2.6Al-0.4Si alloy. (a) The high-resolution image showing the phase. (b) The fast Fourier transform (FFT) of the selected region in (a). (c) is the Mg-based [10,10] crystal band axis diffraction pattern obtained from the (b) spectrum. (d) The diffraction pattern of the precipitated phase stripped from the b-map.

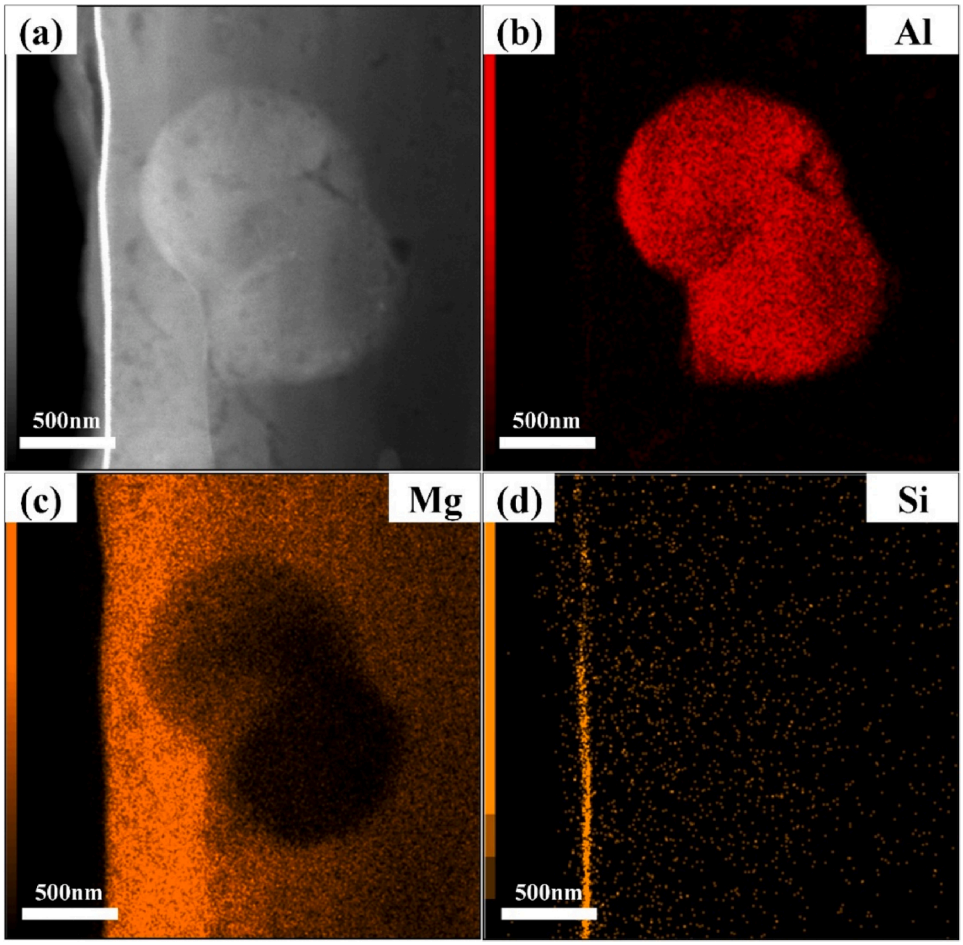

Fig. 8. Energy-dispersive X-ray spectroscopy mapping results of the as-annealed Mg-7Li-2.6Al-0.4Si alloy. (a) SEM morphology. (b) Al element. (c) Mg element. (d) Si element.

dispersed Mg-Si、Mg-Al and Al-Li precipitates could effectively pin the grain boundaries of the α-Mg grains of Mg-7Li-2.6Al-0.4Si alloy, largely restricting the grain recrystallization. It is because of this limited recrystallization activity that the grains in Mg-7Li-2.6Al-0.4Si alloy can be kept very fine. The deformed grains-dominated microstructure is also related to the deformation processing, i.e., casting + extrusion, which is important for the generation of enhanced mechanical properties.

The pole figures of the Mg-7Li-2.6Al-0.4Si alloy are shown in Fig. 6, in which the projections of alloy on the (0001), (11–20) and (10−10) crystal surface exponents are illustrated. The results indicated a strong texture with a maximum intensity value of 31.18, and the maximum value in the pole figure shifted from the basal towards the ED direction. For Mg-xLi alloys, the texture is usually strong at basal plane with a smaller maximum value [25,30]. The results of EBSD data indicate that the addition of Al and Si changed the grain orientation and strengthened the texture intensity of Mg-7Li.

In order to further study the precipitated phase in Mg-7Li-2.6Al-0.4Si alloy, high resolution TEM (HRTEM) examination was performed at one of the precipitates and the result is shown in Fig. 7. Fig. 7(a) shows the diffracted pattern of the precipitate shown in Fig. 3(d), and Fig. 7(b) is the corresponding fast Fourier transform (FFT) diagram of the selected area of the rectangle frame. It can be seen from Fig. 7(b) that there are two sets of spots, and the two sets of spots are separated to obtain the Mg-based [10,10] crystal band axis diffraction (Fig. 7(c)) and the diffraction of the new phase (Fig. 7(d)). For the newly generated phase, the interplanar spacing of speckle in the two directions indicated by the white line is 1.414 nm and 0.5087 nm, respectively. As we know that the precipitates are constituted by phases made up by Mg、Al、Li、Si elements. Among the suspected phases, the Al_2Li_3 was reported to have a similar interplanar spacing of 1.42 nm (ICSD-Demo-ID: 57,951) {001} (d(001)) =1.42 nm) [26]. Therefore, it is confirmed that the precipitates have Al_2Li_3 Phase. The formation of Al_2Li_3 precipitate phase, as also revealed in other study [25,34], could largely strengthen the Mg-7Li-2.6Al-0.4Si alloy.

Fig. 8 presents the EDS mapping results of the precipitate shown in Fig. 7. The precipitate has a size of around 500 nm with a near-spherical shape, and Al is the main component. As we know that Li element is not easily detected by EDS due to the lightweight, thus the precipitate is suspected to be Al-Li phase, which is reasonable if we consider the results shown in Fig. 7. There are also fine rod-shaped Si precipitates at the interface. These precipitates largely contribute to the improved strength and ductility of the designed Mg-7Li-2.6Al-0.4Si alloy.

Therefore, the microstructural characterization results demonstrated that the addition of Al-Si eutectic alloy into Mg-7Li and deformation processing could result in the formation of different types of precipitates: Mg_2Si, AlLi, Al_2Li_3 and $Al_{0.65}Mg_{0.35}$, and the grain refinement with an average grain size of 5.24 μm as well, which all contribute to the simultaneously improved strength and ductility.

3.3. *Fracture morphology*

To uncover the fracturing mechanism of the newly designed Mg-7Li-2.6Al-0.4Si alloy, the crack morphology of Mg-7Li-2.6Al-0.4Si alloy is depicted in Fig. 8, and the crack morphology of Mg-7Li alloy is used as a comparison. Fig. 8(a–c) and Fig. 8(d–f) show the fracture features of Mg-7Li and Mg-7Li-2.6Al-0.4Si alloys, respectively. In Fig. 8(a), lamellar

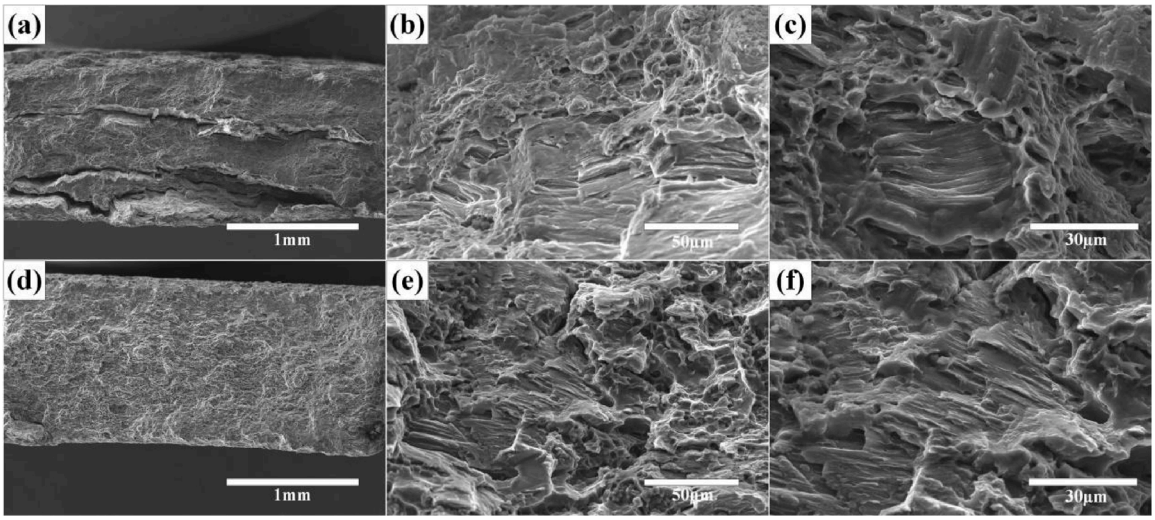

Fig. 9. Crack morphology of Mg-7Li and Mg-7Li-2.6Al-0.4Si alloys under different magnifications. (a-c) Mg-7Li alloy. (d-f) Mg-7Li-2.6Al-0.4Si alloy.

tearing ridge fracture of the Mg-7Li alloy can be clearly observed, which is induced by the large grains which are first dissociated and then fractured under the stretching condition. Fig. 8(b) displays the structure of the non-dissociation area of Mg-7Li alloy where there were dimples shaped in BCC of β-phase, with an elongation of 11 %, as well as muscle patterns in HPC of α-phase, with a tensile strength of 189 MPa. Fig. 8(c) further presents the features of the muscle pattern in Mg-7Li alloy. For Mg-7Li-2.6Al-0.4Si alloy, Fig. 8(d) shows an even fracture without a noticeable lamellar tearing ridge. In Fig. 8(e), besides the dimples and muscle patterns, the river-like transition between them is observed forMg-7Li-2.6Al-0.4Si alloy. It is this dimple + muscle pattern + river-like transition structure contributing to the good alloy plasticity as well as high strength. Therefore, the Mg-7Li-2.6Al-0.4Si alloy was ultralight with excellent comprehensive mechanical properties. Samples of Mg-Li alloys with single α-phase and single β-phase have been previously reported [35–37]. In this study, for the first time, the dimple + muscle pattern + river-like transition is identified as the key structure responsible for producing the ultralight Mg-Li alloy with desirable mechanical properties (Fig. 9).

4. Conclusions

In this paper, a new Mg-7Li-2.6Al-0.4Si alloy has been designed and fabricated. Based on the mechanical testing and microstructural characterization, the simultaneously enhanced mechanical strength and ductility were achieved for this newly designed alloy, and the underlying strengthening and toughing mechanism were revealed.

1. The addition of Al-Si eutectic alloy leads to the significant increase in ultimate tensile strength, yield strength and fracture elongation. The UTS, YS and FE of as-annealed Mg-7Li-2.6Al-0.4Si alloy reached 250 MPa, 192 MPa, and 22 % respectively, which were much higher than the corresponding values for as-annealed Mg-7Li alloy (168 MPa, 148 MPa and 11 %, respectively).

2. The enhanced mechanical properties of Mg-7Li-2.6Al-0.4Si alloy were attributed to the precipitates and refined grains. The precipitates were demonstrated to include $Al_{0.65}Mg_{0.35}$、AlLi、Al_3Li_2 and Mg_2Si phases. The mixed crystal structure, i.e., fine grain-dominated mixed crystal structure with coarse grains allows the alloy to maintain high strength while still having a good elongation.

3. The fracture morphology demonstrated a dimple + muscle pattern + river-like transition structure for Mg-7Li-2.6Al-0.4Si alloy, which is important for the enhanced mechanical performance of the alloy.

Author contributions

Zilong Zhao, Junxian Chen - Conducted the experiments.
Xin Wu, Faqian Liu - Supervised the project.
All authors contributed to data analysis, paper writing, and revising.

Declaration of Competing Interest

The authors declare that they have no known competing financial interests or personal relationships that could have appeared to influence the work reported in this paper.

Acknowledgements

This work was supported by Fuzhou Scholarship Council of China (No. 0020-510819) and the Natural Science Foundation of China (51805086, 51975123). The authors are grateful for the valuable comments from anonymous referees.

References

[1] L.P. Bian, Y.L. Zhao, Y.C. Zhou, T. Wang, L.P. Wang, W. Liang, Effect of Al-Sr master alloy on the formation of long period stacking ordered phase and mechanical properties of Mg-Gd-Zn alloy, Mater. Des. A. 738 (2018) 125–134.
[2] C. Taltavull, Z. Shi, B. Torres, J. Rams, A. Atrens, Influence of the chloride ion concentration on the corrosion of high-purity Mg, ZE41 and AZ91 in buffered Hank's solution, J. Mater. Sci. Mater. Med. 25 (2014) 329–345.
[3] A. Atrens, M. Liu, N.I.Z. Abidin, Corrosion mechanism applicable to biodegradable magnesium implants, Mater. Sci. Eng. B. 176 (2011) 1609–1636.
[4] N.I.Z. Abidin, B. Rolfe, H. Owen, J. Malisano, D. Martin, J. Hofstetter, P. J. Uggowitzer, A. Atrens, The in vivo and in vitro corrosion of high-purity magnesium and magnesium alloys WZ21 and AZ91, Corros. Sci. 75 (2013) 354–366.
[5] C. Taltavull, Z. Shi, B. Torres, J. Rams, A. Atrens, Influence of the chloride ion concentration on the corrosion of high-purity Mg, ZE41 and AZ91 in buffered Hank's solution, Mater. Sci. Mater. Med. 25 (2014) 329–345.
[6] H. Hornberger, S. Virtanen, A.R. Boccaccini, Biomedical coatings on magnesium alloys-A review, Acta Biomater. 8 (2012) 2442–2455.
[7] J. Kuhlmann, I. Bartsch, E. Willbold, S. Schuchardt, O. Holz, N. Hort, et al., Fast escape of hydrogen from gas cavities around corroding magnesium implants, Acta Biomater. 9 (2013) 8714–8721.
[8] N.V. Dudamell, I. Ulacia, F. Galvez, S. Yi, J. Bohlen, D. Letzig, I. Hurtado, M. T. Perz-Prado, Influence of texture on the recrystallization mechanisms in an AZ31 Mg sheet alloy at dynamic rates, Mater. Sci. Eng. A. 532 (2012) 528–535.
[9] B.L. Mordike, T. Ebert, Magnesium: properties-applications-potential, Mater. Sci. Eng. A. 302 (2001) 37–45.
[10] W. Luo, S. Sickafoose, Thermodynamic and structural characterization of the Mg-Li-N-H hydrogen storage system, J. Alloys. Compd. 407 (2006) 274–281.
[11] D.K. Xu, B.J. Wang, C.Q. Li, T.T. Zu, E.H. Han, Effect of icosahedral phase on the thermal stability and ageing response of a duplex structured Mg-Li alloy, Mater. Des. 69 (2015) 124–129.

[12] D.K. Xu, C.Q. Li, B.J. Wang, E.H. Han, Effect of icosahedral phase on the crystallographic texture and mechanical anisotropy of duplex structured Mg-Li alloys, Mater. Des. 88 (2015) 88–97.
[13] T.C. Chang, J.Y. Wang, C.L. Chu, S. Lee, Mechanical properties and microstructures of various Mg-Li alloys, Mater. Lett. 60 (2006) 3272–3276.
[14] R. Wu, Y. Yan, G. Wang, L.E. Murr, W. Han, Z. Zhang, M. Zhang, Recent progress in magnesium-lithium alloys, Int. Mater. Rev. 60 (2015) 65–100.
[15] Y. Zou, L. Zhang, Y. Li, H.T. Wang, J.B. Liu, P.K. Liaw, et al., Improvement of mechanical behaviors of a superlight Mg-Li base alloy by duplex phases and fine precipitates, J. Alloys. Compd. 735 (2017) 2625–2633.
[16] W.Q. Xu, N. Birbilis, G. Sha, Y. Wang, J.E. Daniels, Y. Xiao, M. Ferry, A high-specific-strength and corrosion-resistant magnesium alloy, Nat. Mater. 52 (2015) 1229–1236.
[17] Y. Han, D. Shao, B.A. Chen, Z. Peng, Z.X. Zhu, Q. Zhang, et al., Effect of Mg/Si ratio on the microstructure and hardness-conductivity relationship of ultrafine-grained Al-Mg-Si alloys, J. Mater. Sci. 52 (2017) 4445–4459.
[18] J.L. Gong, W. Liang, H.X. Wang, X.G. Zhao, L.P. Bian, Microstructure and mechanical properties of Mg-12Al- 0.7Si magnesium alloy processed by equal channel angular pressing, J. Rare Metal Mater Eng. 42 (2013) 1800–1804.
[19] Y.H. Kim, J.H. Kim, H.S. Yu, J.W. Choi, H.T. Son, Microstructure and mechanical properties of Mg-xLi-3Al-1Sn-0.4Mn alloys (x=5,8 and 11wt%), J. Alloys Comp. 583 (2014) 15–20.
[20] A. Sanchagrin, R. Tremblay, R. Angers, D. Dube, Mechanical properties and microstructure of new magnesium lithium base alloys, Mater. Sci. Eng. A 220 (1996) 69–77.
[21] Q. Shi, L. Bian, W. Liang, Z. Chen, F. Yang, Y. Wang, Effects of adding Al-Si eutectic alloy and hot rolling on microstructures and mechanical behavior of Mg-8Li alloys, J. Alloys. Compd. 631 (2015) 129–132.
[22] Z.L. Zhao, X.G. Xing, Y. Luo, Y.D. Wang, W. Liang, Influence of Al-Si additions on mechanical properties and corrosion resistance of Mg-8Li dual-phase alloys, J. Iron. Steel. Res. Int. 24 (2017) 426–429.
[23] J. Zhao, J. Fu, A. Tang, H. Sheng, T. Yang, G. Huang, D. Zhang, F. Pan, Influence of Li addition on the microstructures and mechanical properties of Mg-Li alloys, Met. Mater. Int. (2019).
[24] T. Mineta, H. Sato, Simultaneously improved mechanical properties and corrosion resistance of Mg-Li-Al alloy produced by severe plastic deformation, Mater. Sci. Eng. A 735 (2018) 418–422.
[25] C. Zhang, L. Wu, Z.L. Zhao, Z.H. Xie, G.S. Huang, L. Liu, et al., Effect of Li content on microstructure and mechanical property of Mg-xLi-3(Al-Si) alloys, Trans. Nonferrous Met. Soc. China 29 (2019) 2506–2513.
[26] Z.L. Zhao, Z.W. Sun, W. Liang, Y.D. Wang, L.P. Bian, Influence of Al and Si additions on the microstructure and mechanical properties of Mg-4Li alloys, Mater. Sci. Eng. A. 702 (2017) 206–217.
[27] Q. Peng, Y. Sun, B. Ge, H. Fu, Q. Zu, X. Tang, J. Huang, Interactive contraction nanotwins-stacking faults strengthening mechanism of Mg alloys, Acta Mater. 169 (2019) 36–44.
[28] T. Liu, S.D. Wu, S.X. Li, P.J. Li, Microstructure evolution of Mg-14% Li-1% Al alloy during the process of equal channel angular pressing, Mater. Sci. Eng. A. 460 (2007) 499–503.
[29] Z. Drozd, Z. Trojanova, S. Kudela, Deformation behavior of Mg-Li-Al alloys, J. Alloys. Compd. 378 (2004) 192–195.
[30] C. Zhang, L. Wu, Z. L. Zhao, G. S. Huang, B. Jang, A. Atrens, F. S. Pan, Effect of the Al–Si eutectic on the microstructure and corrosion behavior of the single-phase Mg alloy Mg-4Li, J. Magnesium Alloys. Accepted article.
[31] R. Wu, Y. Yan, G. Wang, L.E. Murr, W. Han, Z. Zhang, M. Zhang, Recent progress in magnesium-lithium alloys, Int. Mater. Rev. 60 (2015) 65–100.
[32] J. Tarasiuk, Ph. Gerber, B. Bacroix, Estimation of recrystallized volume fraction from EBSD data, Acta Mater. 50 (2002) 1467–1477.
[33] S. Tang, T. Xin, W. Xu, D. Miskovic, G. Sha, Z. Quadir, et al., Precipitation strengthening in an ultralight magnesium alloy, Nat. Commun. 10 (2019), 2041-1723.
[34] N.C. Goel, J.R. Cahoon, The Al-Li-Mg system (Aluminum-Lithium-Magnesium), Bull. Alloy. Phase Diagr. 11 (1990) 528–546.
[35] C. Liu, P. Shanthraj, J.D. Robson, M. Diehi, D. Raabe, On the interaction of precipitates and tensile twins in magnesium alloys, Acta Mater. 178 (2019) 146–162.
[36] A.A. Nayeb-Hashemi, J.B. Clark, A.D. Pelton, The Li-Mg (Lithium-Magnesium) system, J. Phase Equilibria Diffus. 5 (1984) 365–374.
[37] B. Bo, Y.C. Xin, X.X. Huang, P. Wu, Q. Liu, Quantitative prediction of texture effect on Hall–Petch slope for magnesium alloys, Acta Mater. 173 (2019) 142–152.